# The Alpine metamorphic evolution of the Banchetta-Rognosa and Albergian units (upper Chisone valley, Western Alps)


## Alberto Corno[1]

[1] University of Torino, Earth Sciences Department, via Valperga Caluso 35, 10125, Torino.

AC, 0000-0003-1041-6758.



Rend. Online Soc. Geol. It., Vol. 61 (2023), pp. 10-16, 4 figs. https://doi.org/10.3301/ROL.2023.41

**Short note**

Corresponding author e-mail: alberto.corno@unito.it

*Citation:* Corno A. (2023) - Background contaminants values in groundwater: methodological analysis in the case study of Turin plain (NW Italy). Rend. Online Soc. Geol.It., 61, 10-16, https://doi.org/10.3301/ROL.2023.41.

*Guest Editor:* Martina Casalini

*Submitted:* 14 November 2022

*Accepted:* 28 May 2023

*Published online:* 18 October 2023




SOCIETÀ GEOLOGICA ITALIANA

FONDATA NEL 1881 - ENTE MORALE R. D. 17 OTTOBRE 1885


## ABSTRACT

**This paper deals with the alpine tectono-metamorphic evolution of the Banchetta-Rognosa unit (BRU) and its surrounding Albergian unit (AU), outcropping in the upper Chisone valley (axial sector of the Western Alps). The peak P-T conditions of these two units were defined through the isochemical phase diagram approach. The results of phase equilibria modeling point to eclogite-facies conditions for the BRU (20-23 kbar and 450-520 °C), and lawsonite blueschist-facies conditions for the AU (18-21 kbar and 380-430 °C). Within the Alpine axial sector, where a decrease of the metamorphic condition is recorded form east to west, the BRU could be one of the westernmost eclogite-facies unit. Moreover, its occurrence embedded within the blueschist-facies AU could be the result of complex exhumation processes.**


**KEY-WORDS:** petrography, thermodynamic modeling, Chisone valley, Ligurian-Piedmont Zone, Western Alps.

## INTRODUCTION

The Alpine collisional belt includes tectonic units belonging to different sectors of two continental paleo-margins (either Adriatic or European) and their interposed Ligurian-Piedmont ocean (i.e., Alpine Tethys). During the alpine orogeny, the units forming the axial sector of the Western Alps experienced different tectono-metamorphic evolutions, recording at a regional scale a progressive westward decrease of the alpine metamorphic peak conditions, from eclogite to sub-greenschist facies (Beltrando et al., 2010; Agard, 2021 for a review ). While the P-T conditions of the eclogite-facies units have been thoroughly investigated by many authors (Groppo et al., 2009, 2019; Angiboust et al., 2012; Gasco et al., 2013; Ghignone et al., 2020, 2022), little is known about the units recording blueschist-facies and blueschist-eclogite transition-facies. Moreover, their peak P-T conditions are poorly constrained and mostly via conventional thermobarometric methods (Agard et al., 2001; Beyssac et al., 2002).

Based on some of the results obtained during the PhD project of the Author (Corno et al., 2021a, 2021b and 2022), this work compares the tectono-metamorphic evolution of two units juxtaposed in the tectonic pile exposed in the upper Chisone valley (Western Alps, Fig. 1a-b), namely the Banchetta-Rognosa unit (BRU hereafter) and the Albergian unit (AU hereafter). This comparison represents a useful starting point for any conceptual model that aims to understand the subduction/exhumation processes in this sector of the Western Alps, in the eclogite-blueschist facies transition zone.

The BRU, consisting of continental and oceanic rock successions, is thought to belong to an ocean-continent transition zone (Corno et al., 2019, 2021a) and it is surrounded by different Ligurian-Piedmont oceanic units of the Penninic domain, mainly made of thick sequences of calcschist and minor meta-ophiolitic bodies, from metric to kilometric in size (e.g., Agard, 2021). In particular, the BRU is tectonically embedded within the widespread Albergian unit, belonging to the Ligurian-Piedmont zone.

The peak P-T conditions of these two units were defined through the isochemical phase diagram approach (i.e., P-T pseudosections; Corno et al., 2021b and Corno et al., 2022). For both units, peak P-T conditions were modeled using Perple_X (Connoly, 1990, 2005, 2009), the internally consistent thermodynamic database of Holland & Powell (2011) (ds62), and the equation of state for $H_2O$ of Holland & Powell (1998). Moreover, P-T conditions were further constrained using the predicted stability fields of the observed assemblages, combined with the intersection of compositional isopleths. Bulk rock compositions of rock samples were calculated by combining the mineral proportions obtained from the quantitative modal estimate of SEM-EDS multispectral maps with single-point analyses.

## THE BANCHETTA-ROGNOSA TECTONIC UNIT

The BRU is a small unit (10 km$^2$) consisting of two successions, respectively recording the Mesozoic tectono-depositional evolution of (i) a continental margin, i.e., M. Banchetta succession (Fig. 2a), and (ii) a neighboring oceanic sector, i.e., P. Rognosa succession. Both the successions of the BRU are covered by the same post-rift calcschist. Distinctive features of the BRU are the occurrence of continental-derived clasts in oceanic meta-breccia (suggesting the occurrence and dismantling of continental crust adjacent to exhumed mantle) and Cr-white mica in the matrix of continental meta-breccia (interpreted as signature of deposition in sectors proximal to areas floored by exhumed mantle). This peculiar setting suggests pre-orogenic proximity (i.e., juxtaposition) of continental- and oceanic-derived rocks at the hyperextended European distal margin (Corno et al., 2021a).

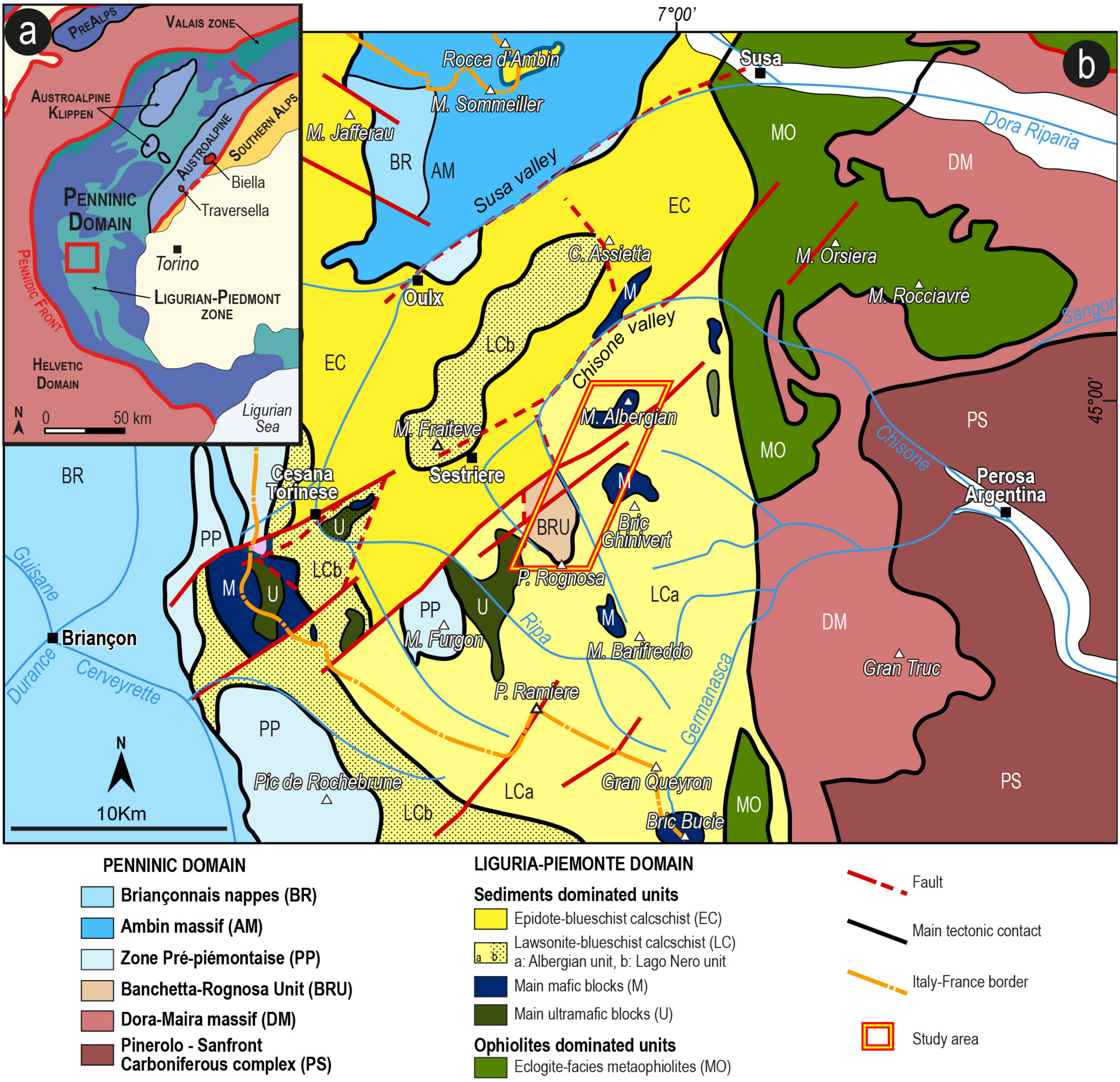


Fig. 1 - a. Simplified tectonic map of the Western Alps (redrawn and modified from Bigi et al., 1990); b. Schematic geological map of the upper Susa and Chisone valleys (modified from Corno et al., 2021b).

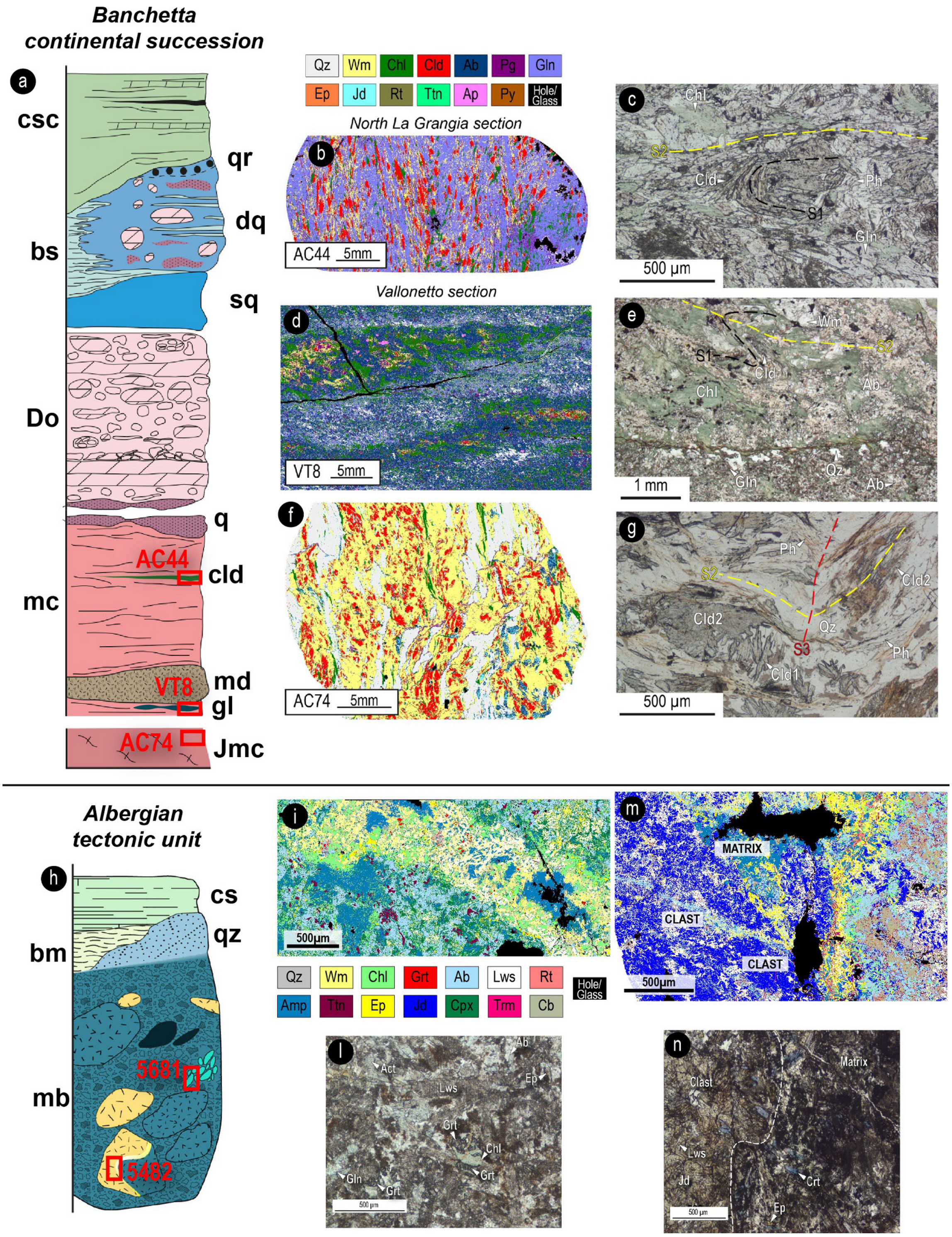


Fig. 2 - a. Simplified lithostratigraphic log of the continental succession of the Banchetta-Rognosa tectonic unit. Red polygons show the approximate positions of the samples used for thermodynamic modeling. Acronyms are: bs, black micaschist; cld, Cld+Ph-bearing glaucophanic schist; csc, calcschist; Do, dolostone sequence; dq, polymictic meta-breccia with quartzite and dolostone clasts within a carbonate matrix; gl, Cld-bearing glaucophanite layer; Jmc, Jd-bearing gneissic micaschist; mc, micaschist; md, Grt-bearing metabasite body; q, quartzite body; qr, discontinuous meta-sandstone body with dolostone clasts; sq, carbonate-bearing quartzite; b. Processed X-ray maps of sample AC44, Cld+Ph-bearing glaucophanic schist from Corno et al., 2021b; c. Sample AC44, polygonal arc of chloritoid crystals, with S2 axial plane schistosity defined by phengite+glaucophane (Plane Polarized Light, PPL), from Corno et al., 2021b; d. Processed X-ray maps of sample VT8, Cld-bearing glaucophanite from Corno et al., 2021b; e. Sample VT8, relict S1 foliation almost completely replaced by white mica (=Wm)+chlorite+albite S2 axial plane schistosity (PPL), from Corno et al., 2021b; f. Processed X-ray maps of sample AC74, Jd-bearing gneissic micaschist from Corno et al., 2021b; g. Sample AC74, first generation of chloritoid crystals (Cld1) preserved in a microlithon wrapped by S2 main foliation, defined by a second generation of chloritoid (Cld2)+phengite+quartz (PPL), from Corno et al., 2021b; h. Simplified lithostratigraphic log of the Albergian tectonic unit of the Ligurian-Piedmont zone. Red polygons show the approximate positions of the samples used for thermodynamic modeling. Acronyms are: bm, black micaschist; cs, calcschist qz, quartzitic meta-sandstone; mb, mafic meta-breccia kilometric body, with yellowish Mg-Al gabbro clasts, dark blue Fe-Ti gabbro clasts, light blue plagiogranite clasts; i. Processed X-ray maps of sample 5482, Mg-Al meta-gabbro clast from Corno et al., 2022; l. Sample 5482, anhedral garnet crystals, partially retrogressed by chlorite and epidote (PPL); m. Processed X-ray maps of sample 5681, plagiogranite meta-breccia from Corno et al., 2022; n. Sample 5681, clast-matrix boundary in the plagiogranite metabreccia. Note the widespread occurrence of jadeite crystals, lawsonite, and minor Fe-glaucophane in the clast (left), while the matrix has a more retrogressed mineral assemblage, with a widespread occurrence of epidote-group minerals and crossite (PPL).

The P. Rognosa oceanic succession (Corno et al., 2019), is made of serpentinized mantle overlain by syn-rift polymictic meta-breccia (with both oceanic- and continental- derived clasts) and discontinuous meta-sandstone bodies with dolostone clasts and blocks. The M. Banchetta continental succession of the BRU (Fig. 2a), whose main features can be observed in the Troncea valley, is made of a crystalline basement (with minor polymetamorphic bodies), overlain by scarce levels of quartzite and a thick dolomitic sequence, followed by syn-rift carbonate-bearing quartzite, polymictic meta-breccia with quartzite and dolostone clasts within a carbonate matrix, and black micaschist. Locally, discontinuous meta-sandstone bodies with dolostone clasts occur, quite similar to those occurring in the oceanic succession. The thick post-rift sequence is characterized by calcschist, common to both the Banchetta continental- and Rognosa oceanic succession. For thermodynamic modeling purposes, the study focused on the M. Banchetta continental succession, better preserving the mineral assemblages useful for the isochemical phase diagram approach.

Based on their mineral assemblages, 3 samples have been selected, which are considered as the most suitable for constraining the Alpine HP tectono-metamorphic evolution of the BRU. Sample AC44 is a Cld+Ph-bearing glaucophanic schist (Fig. 2b), characterized by a well-developed main foliation, defined by phengite (Fig. 3a), glaucophane (Fig. 3b), chloritoid and paragonite, derived from the transposition of an earlier schistosity (partially preserved in polygonal arcs and intrafolial folds mainly made of chloritoid and glaucophane crystals; Fig. 2c). While chlorite statically overgrows chloritoid and glaucophane, large muscovite flakes statically overgrow S1- and S2-related phengite. Sample VT8 is a Cld-bearing, partially retrogressed, glaucophanite (Fig. 2d). The main foliation is defined isoriented phengite and paragonite (Fig. 3a), glaucophane (Fig. 3b), chlorite, and chloritoid, and it is derived from the transposition of an older schistosity defined by an earlier generation of glaucophane and chloritoid, still preserved in mm–sized microlithons (Fig. 2e). Static muscovite partially replaces phengite and paragonite, while poikiloblastic albite and quartz+chlorite replace glaucophane. Sample AC74 is a Jd-bearing gneissic micaschist (Fig. 2f), characterized by a main foliation made of white mica (Fig. 3a), chlorite, chloritoid and quartz-rich layers enveloping microlithons with a relict foliation defined by quartz, white micas, chloritoid, jadeite, and rutile (highlighted by polygonal arcs and intrafolial folds; (Fig. 2g). Jadeite porphyroblasts are enveloped by the main foliation and are partially and variably replaced by a fine-grained aggregate of quartz and albite. Late albite, chlorite and muscovite grow statically on the main foliation.

## METHODS AND THERMODYNAMIC MODELING

The peak P–T conditions of the selected samples were constrained using the isochemical phase diagram approach, based on the predicted stability field of the observed assemblages, combined with the intersection of compositional isopleths modelled for chloritoid and glaucophane (samples AC44 and VT8; representative analyses can be found in the supplementary material from Corno et al., 2021b). The isochemical phase diagrams were calculated in the system MnNKFMASOH (MnO-$Na^2O$-$K_2O$-FeO-MgO-$Al_2O_3$-$SiO_2$-$O_2$-$H_2O$) for samples AC44 and AC74 and in the system NKFMASOH ($Na_2O$-K2O-FeO-MgO- $Al_2O_3$-$SiO_2$-$O_2$-$H_2O$) for sample VT8. CaO was neglected because Ca-bearing phases are lacking. TiO2 was not included in the calculation because rutile is the only Ti-bearing phase stable at HP conditions in all the samples. Fluid saturated conditions were assumed (due to the large occurrence of hydrous phases and the absence of primary carbonates and sulphides), and the fluid was considered as pure $H_2O$ ($aH_2O$=1).

## P-T CONDITIONS

Modeled peak P-T conditions are (red ellipses in Fig. 2a): i) 21-22 kbar and 450±25°C for the Cld-Ph bearing glaucophanic schist (AC44); ii) 21-22.5 kbar and 450±20°C for the Cld-bearing glaucophanite (VT8); iii) 21-23 kbar and 470±50°C for the Jd-bearing gneissic micaschist. Hence, based on the intersection of predicted ellipses, common peak P-T conditions can be constrained at 20–23 kbar and 440–500 °C.

## THE ALBERGIAN TECTONIC UNIT

The AU comprises a thick sequence of calcschists wrapping minor meta-ophiolitic bodies, from metric to kilometric in size (Servizio Geologico d'Italia, 2020 with references therein). The AU crops out from the Susa valley (to the North) to the Pellice valley (to the South; Fig. 1). The analyzed meta-mafic body cropping out in the upper Chisone valley (Monte Albergian – Gran Mioul sector) consists of a clast-supported meta-breccia, dominated by metabasite clasts and blocks, with minor doleritic and gabbro clasts (Fig. 2h). In addition, rare meta-plagiogranitic clasts have been found, wrapped by the same mafic matrix. The whole meta-mafic body is covered by discontinuous levels of quarzitic meta-sandstone and and/or discontinuous levels of black micaschist, followed by a thick sequence of calcschist.

P-T isochemical phase diagrams were calculated for a Grt+Omp Mg-Al metagabbro (sample 5482) and a plagiogranitic meta-breccia (sample 5681). Sample 5482 is a fine-grained Mg-Al metagabbro (Fig. 2i), characterized by a banded structure at the micro-scale. Mafic layers consist of Ca-clinopyroxene, actinolite (Fig. 3d), chlorite, albite, and titanite, while sialic layers consist of small garnet (100-200 µm; Fig. 2l), lawsonite, white mica (Fig. 3c), actinolite (Fig. 3d), epidote, and chlorite. Sample 5681 metabreccia is made of plagiogranitic clasts within a mafic matrix (Fig. 2m). Clasts consist mainly of jadeite (47%), and lawsonite, albite, glaucophane, and epidote (Fig. 2n). The mafic matrix consists of albite, glaucophane (Fig. 3d), white mica (Fig. 3c), epidote, lawsonite, chlorite, and quartz (Fig. 2n). Due to the significant difference in bulk compositions, related to different mineral assemblages and proportion, two distinct phase diagrams were calculated, one for the plagiogranitic clasts, and one for the mafic matrix.

## METHODS AND THERMODYNAMIC MODELING

The P-T pseudosection for sample 5482 was calculated in the system MnNCFMASTH (MnO-$Na_2O$-CaO-FeO-MgO-$Al_2O_3$-$SiO_2$-$TiO_2$-$H_2O$). For sample 5681, the P-T pseudosection of the plagiogranitic clasts was calculated in the system NCKFMASTOH ($Na_2O$-CaO-$K_2O$-FeO-MgO-$Al_2O_3$-$SiO_2$-$TiO_2$-$O_2$-$H_2O$), while that for the mafic matrix was calculated in the system NCKFMASTH ($Na_2O$-CaO-$K_2O$-FeO-MgO$Al_2O_3$-$SiO_2$-$TiO_2$-$H_2O$). Representative analyses of the mineral phases occurring in these two samples can be found in the supplementary material from Corno et al. (2022). Fluid saturated conditions were assumed (due to the large occurrence of hydrous phases and the absence of primary carbonates and sulphides), and the fluid was considered as pure $H_2O$ ($aH_2O$=1). MnO was neglected in modeling of sample 5681 because Mn-bearing phases are lacking. $Fe^{3+}$ was neglected in pseudosections of samples 5482 and the matrix of sample 5681, because $Fe^{3+}$-rich oxides are absent and the amount of $Fe^{3+}$ in the analyzed minerals is very low. On the opposite, $Fe^{3+}$ was considered for the clasts of sample 5681, due to the occurrence of acmitic-rich clinopyroxenes.

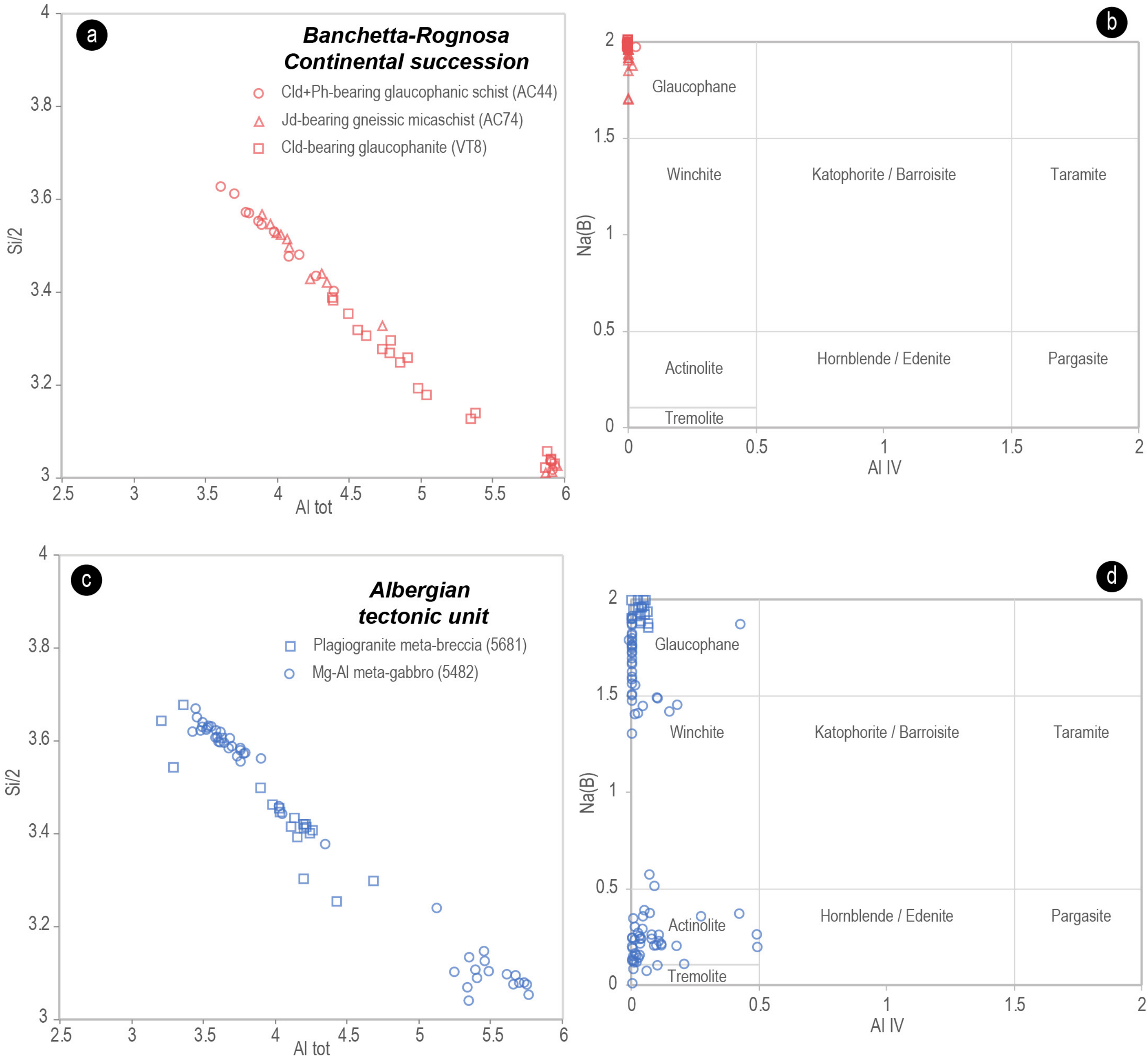


**Fig. 3 - Mineral chemistry and classification diagrams for white mica and amphibole group minerals (for more classifications diagrams see Corno et al., 2021b, and Corno et al., 2022). Continental succession of the Banchetta-Rognosa tectonic unit, a. White mica composition in the Si vs (AlIV + AlVI) diagram for the three selected samples; b. Amphibole composition in the Hawthorne et al. (2012) diagram Na vs AlIV; Albergian tectonic unit, c. White mica composition in the Si vs (AlIV + AlVI) diagram for the two selected samples; d. Amphibole composition in the Hawthorne et al. (2012) diagram Na vs AlIV.**

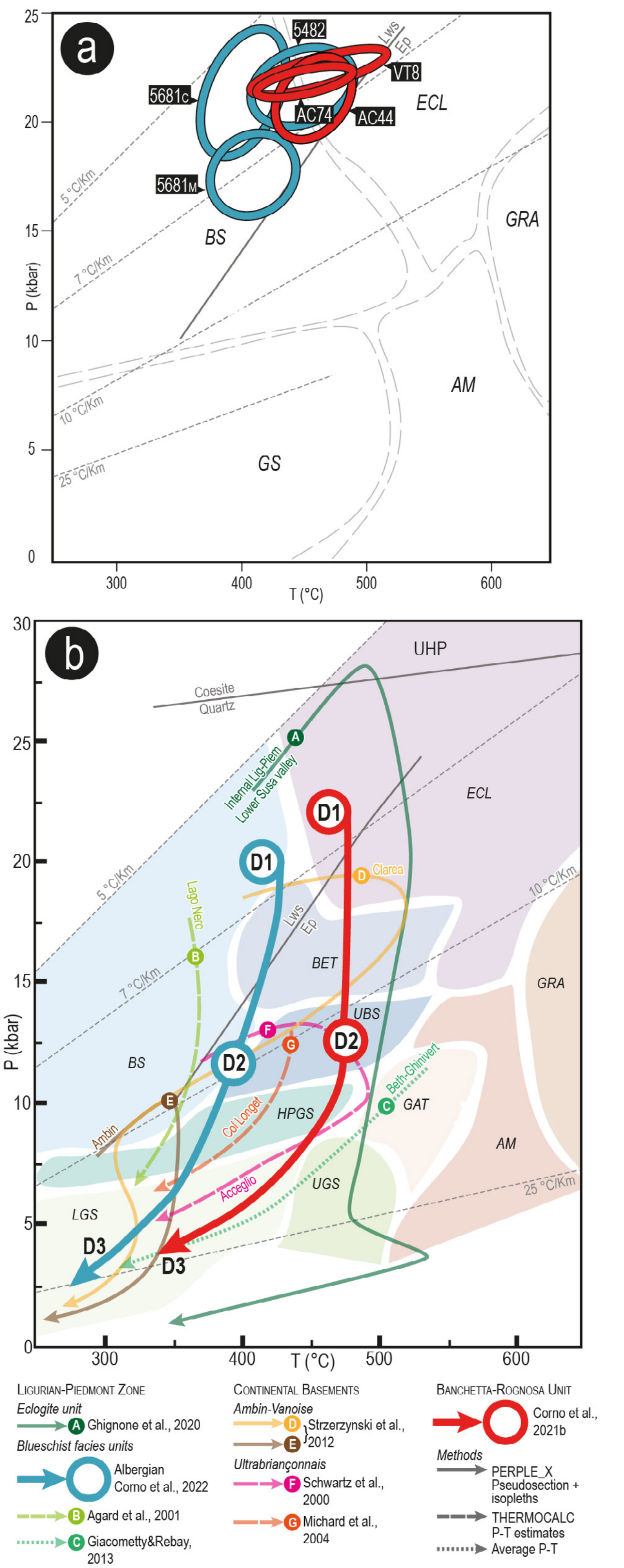


**Fig. 4 - a. Ellipses for constrained P-T conditions for each sample from the Albergian unit (blue ellipses from Corno et al., 2022. C and m for sample 5681 stand for c: clasts and m: matrix) and the Banchetta-Rognosa unit (red ellipses from Corno et al., 2021b). Ellipses are based on the observed mineral assemblages and the intersection of compositional isopleths; b. Compilation of P–T trajectories of different units of the Western Alps for comparison with the studied area. Metamorphic facies diagram redrawn from Bousquet et al., 2008. LGS: low greenschist; UGS: upper greenschist; HPGS: high pressure greenschist; GAT: greenschist-amphibolitic transition; AM: amphibolitic; BS: blueschist; UBS: upper blueschist; GRA: granulitic; BET: blueschist-eclogitic transition; ECL: eclogitic; UHP: ultra-high pressure.**

## P-T CONDITIONS

Modeled peak P-T conditions are (blue ellipses in Fig. 2a): i) 21±1.5 kbar and 450±30°C for the Mg-Al meta-gabbro sample 5482; ii) 18 ± 2 kbar and 410±20°C for the matrix and 21-24 kbar and T < 430°C for the meta-plagiogranitic clasts of sample 5681. Hence, based on the partial overlap of predicted ellipses, common peak P-T conditions can be constrained at 18-20 kbar and 380-420 °C.

## DISCUSSION

The constrained metamorphic peak of the Banchetta-Rognosa unit (20–23 kbar and 440–500 °C), typical of eclogite-facies conditions, is higher than previously believed, as well as higher than that recorded in the embedding blueschist-facies Albergian unit (18-20 kbar and 380-420 °C).

From the comparison in Fig. 2b, it appears that the BRU experienced a metamorphic peak at P–T conditions intermediate between those registered by the eclogite-facies of the Internal Piedmont Zone, to the East (Ghignone et al., 2020), and those registered by the oceanic and continental-derived units classically ascribed to the blueschist-facies metamorphic domain, to the West (Agard, 2021).

This finding suggests that the BRU could be one of the westernmost eclogite-facies unit in the Western Alps, therefore extending the eclogite-facies metamorphic domain toward the west. The current emplacement of the BRU within the (slightly) lower grade AU can be tentatively explained taking into account a trans-tensional tectonic regime during late Alpine evolution (e.g., Tricart & Sue, 2006; Tricart et al., 2007). However, further investigations are needed in order to constrain the complex exhumation processes involved in the Alpine orogeny.

## AKNOWLEDGEMENTS

Borghi A., Gattiglio M., and Groppo C. are greatly acknowledged for their contributions in the production of the papers reviewed in this work. A special thanks goes to Mosca P. for having read a first draft of this work and his insightful comments. I'm thankful to M. Berti for his editorial job.

## REFERENCES

Agard P. (2021) - Subduction of oceanic lithosphere in the Alps: Selective and archetypal from (slow-spreading) oceans. Earth-Science Reviews, 103517.

Agard P., Vidal O. & Goffé B. (2001) - Interlayer and Si content of phengite in HP–LT carpholite-bearing metapelites. J. Metam. Geol., 19(5), 479-495.

Angiboust S., Langdon R., Agard P., Waters D. & Chopin C. (2012) - Eclogitization of the Monviso ophiolite (W. Alps) and implications on subduction dynamics. Journal of Metamorphic Geology, 30(1), 37-61.

Beltrando M., Compagnoni R. & Lombardo B. (2010) - (Ultra-) High-pressure metamorphism and orogenesis: An Alpine perspective. Gondwana Res., 18(1), 147-166.

Beyssac O., Rouzaud J. N., Goffé B., Brunet F. & Chopin C. (2002) - Graphitization in a high-pressure, low-temperature metamorphic gradient: A Raman microspectroscopy and HRTEM study. Contributions to Mineralogy and Petrology, 143, 19-31.

Bigi G., Castellarin A., Coli M., Dal Piaz G.V., Sartori R., Scandone P. & Vai G.B. (1990) - Structural Model of Italy scale 1:500.000, sheet 1. C.N.R., Progetto Finalizzato Geodinamica, SELCA Firenze.

Bousquet R., Oberhänsli R., Goffé B., Wiederkehr M., Koller F., Schmid S. M., Schuster R., Engi M., Berger A. & Martinotti G. (2008) - Metamorphism of metasediments at the scale of an orogen: A key to the Tertiary geodynamic evolution of the Alps. Geological Society, London, Special Publications, 298(1), 393-411

Connolly J.A.D. (1990) - Multivariable phase diagrams: An algorithm based on generalized thermodynamics. Am. J. Sci., 290, 666-718.

Connolly J.A.D. (2005) - Computation of phase equilibria by linear programming: A tool for geodynamic modeling and its application to subduction zone decarbonation. Earth Planet. Sci. Lett., 236 (1-2), 524-541.

Connolly J.A.D. (2009) - The geodynamic equation of state: What and how. Geochem., Geophys. Geosyst., 10 (10), 1-19.

Corno A., Mosca P., Borghi A. & Gattiglio M. (2019) - Lithostratigraphy and petrography of the Monte Banchetta-Punta Rognosa oceanic succession (Troncea and Chisonetto Valleys, Western Alps). Ofioliti, 44(2), 83-95.

Corno A., Mosca P., Gattiglio M. & Borghi A. (2021a) - Geological map of the Monte Banchetta – Punta Rognosa area (Troncea valley, Western Alps). J. Maps, 17(2), 150-160.

Corno A., Groppo C., Mosca P., Borghi A. & Gattiglio M., 2021b) - Eclogitic metamorphism in the Alpine far-west: petrological constraints on the Banchetta-Rognosa tectonic unit. Swiss J. Geosci., 114, 16.

Corno A., Mosca P., Groppo C., Borghi A. and Gattiglio M. (2022) - More widespread than supposed: preserved lawsonite in the blueschist-facies ophiolitic bodies from the Albergian unit (Liguria-Piemontezone, Western Alps). Ofioliti, 47(2).

Gasco I., Gattiglio M. & Borghi A. (2013) - Review of metamorphic and kinematic data from Internal Crystalline Massifs (Western Alps): PTt paths and exhumation history. Journal of Geodynamics, 63, 1-19.

Ghignone S., Borghi A., Balestro G., Castelli D., Gattiglio M. & Groppo C. (2020) - HP tectono-metamorphic evolution of the Internal Piedmont Zone in Susa Valley (Western Alps): New petrologic insight from garnet+chloritoid-bearing micaschists and Fe–Ti metagabbro. J. Metam. Geol., 39(4), 391-416.

Ghignone S., Scaramuzzo E., Bruno M. & Livio F. (2022) - A new UHP unit in the Western Alps: first occurrence of coesite from the Monviso Massif (Italy). American Mineralogist, in press.

Giacometti F. & Rebay G. (2013) - Structural and petrological evolution of the Beth-Ghinivert zone (Schistes Lustres—Italian Western Alps). Rendiconti Online Soc. Geol. Ital., 29, 70-73.

Groppo C., Beltrando M. & Compagnoni R. (2009) - P-T path of the UHP Lago di Cignana and adjoining HP meta-ophiolitic units: Insights into the evolution of subducting tethyan slab. Journal of Metamorphic Geology, 27, 207–231.

Groppo C., Ferrando S., Gilio M., Botta S., Nosenzo F., Balestro G., Festa A. & Rolfo F. (2019) - What's in the sandwich? New P-T constraints for the (U)HP nappe stack of southern Dora-Maira Massif (Western Alps). European Journal of Mineralogy, 31(4), 665-683.

Hawthorne F.C., Oberti R., Harlow G.E., Maresch W.V., Martin R.F., Schumacher J.C. and Welch M.D., (2012) - Nomenclature of the amphibole supergroup. Am. Miner., 97 (11-12): 2031-2048.

Holland T.J.B. and Powell R., (1998) - An internally consistent thermodynamic dataset for phases of petrological interest. J. Metam. Geol., 16, 309-343.

Holland T.J.B. and Powell R., (2011) - An improved and extended internally consistent thermodynamic dataset for phases of petrological interest, involving a new equation of state for solids. J. Metam. Geol., 29, 333-383.

Michard A., Avigad D., Goffé B. & Chopin C. (2003) - The high-pressure metamorphic front of the south Western Alps (Ubaye-Maira transect, France, Italy). Schweiz. mineral. petro. Mitt., 84, 215-235.

Schwartz S., Lardeaux J. M. & Tricart P. (2000) - La zone d'Acceglio (Alpes Cottiennes). Un nouvel exemple de croûte continentale éclogitisée dans les Alpes occidentales. C. R. Acad. Sci., 330, 859-866.

Servizio Geologico d'Italia, (2020) - Carta Geologica d'Italia alla scala 1:50.0000, F. 171 Cesana. http://www.isprambiente.gov.it/Media/carg/171_CESANA_TORINESE/Foglio.html

Strzerzynski P., Guillot S., Leloup P. H., Arnaud N., Vidal O., Ledru P., Courrioux G. & Darmendrail X. (2012) - Tectono-metamorphic evolution of the Briançonnais zone (Modane-Aussois and southern Vanoise units, Lyon Turin transect, western alps). J. of Geodyn., 56, 55-75.

Tricart P. & Sue C. (2006) - Faulted backfold versus reactivated backthrust: the role of inherited structures during late extension in the frontal Piémont nappes east of Pelvoux (Western Alps). International Journal of Earth Sciences, 95, 827-840.

Tricart P., Van der Beek P., Schwartz S. & Labrin E. (2007) - Diachronous late-stage exhumation across the western Alpine arc: constraints from apatite fission-track thermochronology between the Pelvoux and Dora-Maira Massifs. Journal of the Geological Society, 164(1), 163-174.